COMPDYN 2025
10th ECCOMAS Thematic Conference on
Computational Methods in Structural Dynamics and Earthquake Engineering
M. Papadrakakis, M. Fragiadakis (eds.)
Rhodes Island, Greece, 15-–18 June 2025

IMPACT OF GROUND MOTION RECORD SELECTION ON HIGHER-MODE RESPONSES IN RC WALL BUILDINGS: COMPARING UNIFORM HAZARD AND CONDITIONAL SPECTRA APPROACHES

Jose Poveda[1], and Gerard J. O'Reilly[2]

[1]Centre for Training and Research on Reduction of Seismic Risk (ROSE Centre), Scuola Universitaria Superiore IUSS di Pavia
Pavia 27100, Italy
e-mail: jose.poveda@iusspavia.it

[2] e-mail: gerard.oreilly@iusspavia.it

Keywords: RC walls, higher-modes, ground motions, UHS, conditional spectrum

Abstract. *This research investigates how code-specified methods for selecting ground motion records affect the higher-mode responses in structural analysis. The study contrasts two target spectra: the Uniform Hazard Spectrum (UHS) and the Conditional Spectrum (CS), examining their influence on shear wall buildings designed using Eurocode 8 (EC8) response spectrum analysis. By assessing nonlinear structural responses under different record selection strategies, including UHS alone and different CS with conditional periods beyond the primary mode, we quantify impacts on engineering demand parameters (EDPs) such as peak-storey drift, base shear, and overturning moment. The findings indicate that the UHS approach generally leads to higher EDP values, while using a single CS tends to yield much lower estimates depending on the conditioning period. Although the UHS approach may overpredict demands, it is simpler, requiring fewer records and input specifications compared to CS, which, though more extensive, offers limited gains in higher-mode accuracy. Additionally, inadequate CS selection may vastly underestimate certain EDPs along the structure's height. This study emphasizes the importance of understanding code implications and weighing the trade-offs between the presumed increase in accuracy when using the CS versus the UHS' effectiveness when estimating Higher-Mode Responses in RC Wall Buildings.*

1 Introduction

Reinforced concrete (RC) shear walls play a prominent role in seismic design worldwide, providing essential lateral stiffness, strength, and adaptability, particularly in high-rise buildings. However, events like the 2010 Chile earthquake exposed vulnerabilities in RC shear walls, particularly in lower storeys, due to factors such as high axial stresses, inadequate transverse reinforcement, and vertical irregularities [1]. These issues highlight the limitations of conventional design methods, including pushover analyses, which primarily focus on first-mode responses and fail to account for complex dynamic interactions. This study revisits some fundamental assumptions in ductile shear wall seismic design and verified through ground motion record selection and non-linear dynamic analysis. It explores methods such as Conditional Spectrum (CS) [2] featured in the new generation of Eurocode 8 [3] and compares them with the well-established Uniform Hazard Spectra (UHS) approach. The research begins with a probabilistic seismic hazard analysis (PSHA) to compute hazard curves and UHS for different return periods. The design phase employs the UHS for a 475-year return period as the elastic design spectrum, guiding the design of shear walls in accordance with the current Eurocode 8 (EC8) guidelines [4]. Once the design is complete, disaggregation analysis is performed to derive CS at each return period, and record selection is performed for both methodologies, enabling multiple-stripe analyses to compare engineering demand parameters (EDPs).

2 Case study structures

This study considered the seismic response of five RC shear wall buildings with varying heights of 4, 8, 12, 16, and 20 storeys. Each building featured a typical inter-storey height of 3 metres, a floor area of $600m^2$ from a 20 by 30 meters plan layout, giving a floor mass of 490 tons, including the roof, and four walls of equal length l_w and thickness t_w as shown in Figure 1a and in Figure 1b. A simple equivalent cantilever model was developed in OpenSees for analysis, as shown in Figure 1c, where the cracked section properties followed the Los Angeles Tall Buildings Structural Design Council (LATBSDC) [5] recommendation of 0.6 factor for cracking in bending and 0.75 in shear with respect to the gross elastic stiffnesses.

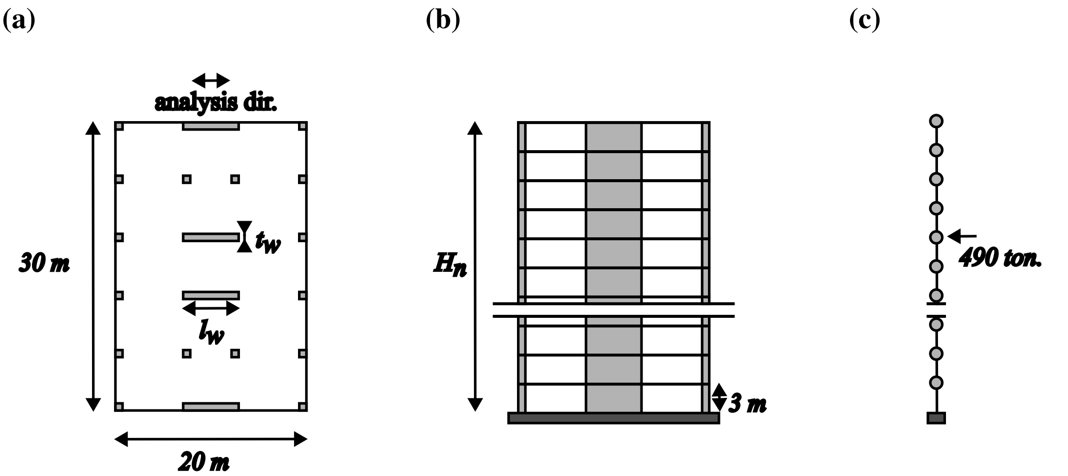

Fig. 1. a) Buildings' plan; b) Buildings' elevation; c) Numerical model

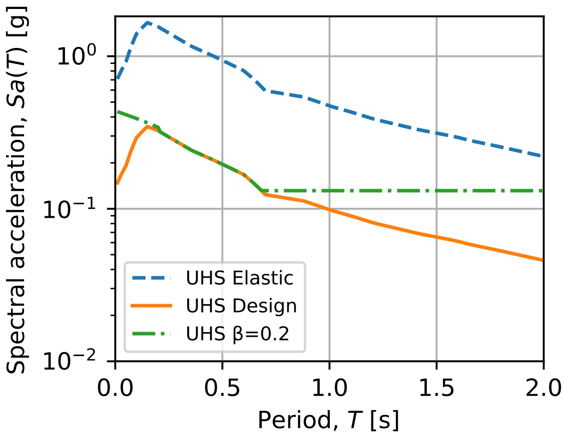

Fig. 2. Elastic and design response spectra

2.1 Seismic design

The buildings were designed as ductile shear walls following EC8 [4]. Response Spectrum Analysis (RSA) using a UHS at 475-year return period spectra was adopted as the design methodology. To estimate the modal properties needed for RSA, the numerical model shown in Figure 1c was used. Table 1 shows the modal periods and mass percentage participation for the first three modes of the linear model for the final designs. The gravity load system's contribution to the building's lateral stiffness was not included. When defining the design spectra for the RSA, the EC8 design rules were applied to the UHS determined from PSHA for a site in Duzce, Turkey. That is, the UHS was divided by the design ductility factor $q = 5.4$ and the design forces were determined as prescribed by EC8. The reason the UHS was adopted instead of the simplified spectrum prescribed by EC8 was to ensure consistency between the designs and the ground motion record selection based on PSHA. The lower bound for the design spectral acceleration $\beta = 0.2$ was also applied to ensure minimum lateral resistance criteria were met, as prescribed by the code. The elastic and design spectra are illustrated in Figure 2.

	4 Storey		8 Storey		12 Storey		16 Storey		20 Storey	
Mode	$T(s)$	$m_{e,i}$ (%)	$T(s)$	m_e, i (%)	$T(s)$	$m_{e,i}$ (%)	$T(s)$	m_e, i (%)	$T(s)$	$m_{e,i}$ (%)
1	0.88	70.3	1.21	65.9	1.41	64.5	1.64	63.7	1.82	63.2
2	0.15	21.9	0.21	21.1	0.24	20.7	0.28	20.3	0.30	20.1
3	0.06	6.32	0.08	7.14	0.09	7.18	0.11	7.13	0.12	7.07

Table 1. Dynamic properties of building model

The RSA demands on the buildings, along with the elastic and design spectral acceleration for the first mode, are summarised in Table 2 for the RSA using the CQC modal combination of all modes, even if only three modes were necessary to reach the 90 % modal mass participation rules. The maximum peak storey drift (PSD) demand was also evaluated and ensured to be below the design threshold of 2%.

Once the RSA results were available, capacity design envelopes were developed to account for the overstrength of the wall at the base, and the effects of higher modes, and the required reinforcement was subsequently sized. Figure 3 shows the design envelopes for the 20-storey

Building	$Sa(T_1)[g]$	$Sa(T_1)Sa/q \geq \beta Sa(T_1)[g]$	Base Shear (MN)	Base Moment (MNm)	Drift (%)
4 Storey	0.543	0.13	2.42	17.98	1.62
8 Storey	0.390	0.13	4.46	63.95	1.17
12 Storey	0.331	0.13	6.37	137.63	0.93
16 Storey	0.283	0.13	8.22	239.12	0.82
20 Storey	0.253	0.13	10.05	368.21	0.72

Table 2. Buildings' demand for design UHS-475 years return period

building and the final strength of the wall once the rebar's spacings and diameters were defined. For simplicity, the final design at the base was assumed constant along the buildings high. Still, it is not uncommon for designers to choose to optimise and reduce rebar provisions along the height. The design properties of each building's wall are summarised in Table 3 and the base shear and overturning moment of the walls from the capacity design envelope are shown in Table 4 along with the ε value from code, needed for the base shear capacity envelope ($V_{Ed,b} = \varepsilon \cdot V'_{Ed,b}$)and the shear overstrength ratio ($V_{Ed,b}/V_n$).

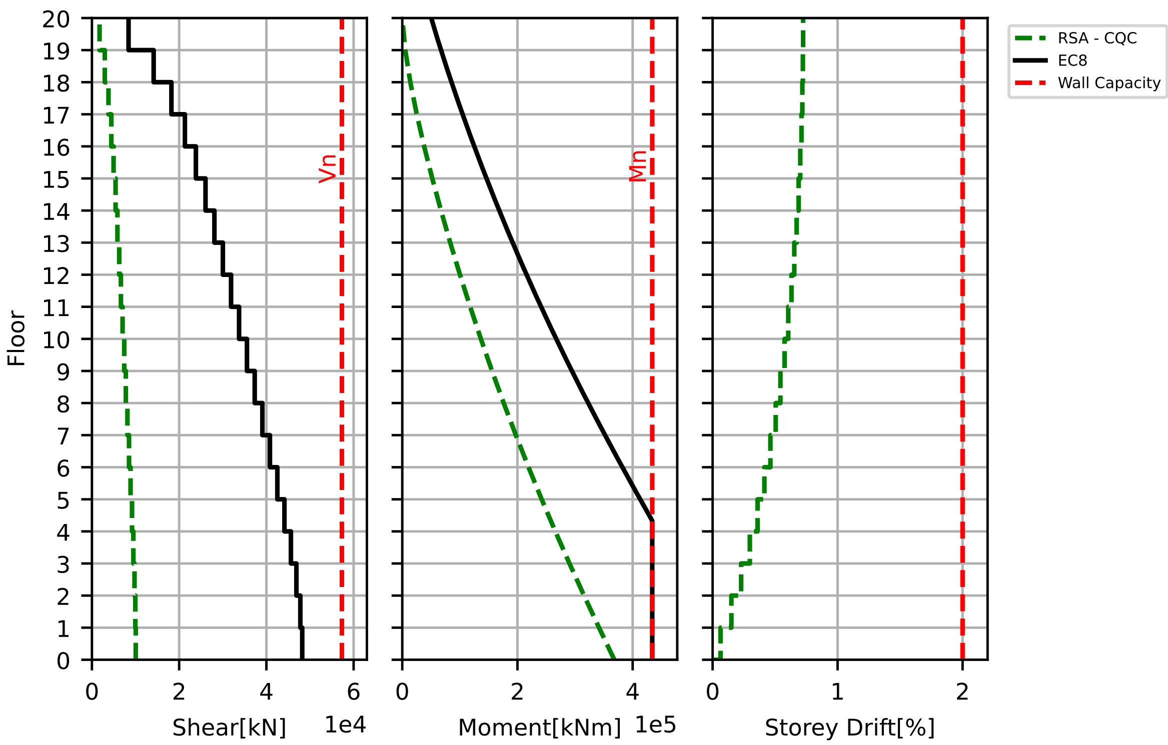

Fig. 3. EC8 capacity design envelope for 20-storey building

2.2 Non-linear modelling

The non-linear model incorporated a lumped plastic hinge at the base of the wall to represent the flexural yielding, using a simple bi-linear hysteretic model *Steel01* provided in OpenSees [6] with a 1% post-yielding stiffness. The plastic hinge length, l_{pl}, and yield curvature, ϕ_y,

Building	H_n (m)	f'_c (MPa)	l_w (m)	t_w (m)	$d_{b,l}$ (mm)	s_l (cm)	ρ (%)	$d_{b,t}$ (mm)	s_t (cm)
4 Storey	12	30	2.50	0.30	12	20	0.37	16	10
8 Storey	24	30	4.50	0.35	12	20	0.32	16	7.5
12 Storey	36	30	6.50	0.40	12	20	0.28	16	7.5
16 Storey	48	50	7.50	0.45	12	20	0.25	20	7.5
20 Storey	60	50	8.50	0.60	14	20	0.25	20	7.5

Table 3. Building design properties

Building	ε	$V_{Ed,b}(MN)$	$V_n(MN)$	$V_{Ed,b}/V_n$	$M_n(MNm)$
4 Storey	2.8	6.9	7.29	1.06	26.5
8 Storey	3.5	15.87	17.70	1.12	90.7
12 Storey	4.0	25.80	26.60	1.03	193.1
16 Storey	4.5	37.21	47.36	1.27	278.8
20 Storey	4.8	48.22	57.32	1.19	434.0

Table 4. Building walls strength and shear over-strength ratio

were calculated based on wall geometry using the relationship for rectangular walls described in Priestley et al. [7]. The parameters for defining the plastic hinge are summarised in Table 5.

P-delta effects were incorporated using a corotational element, with the vertical load of each floor's weight applied to the end nodes of the columns. A constant modal damping ratio of $\xi = 5\%$ was assumed for all modes, despite modern recommendations for lower values, such as those in LATBSDC [5]. Finally, the model did not account for shear failure or shear-flexural interaction.

3 Analysis

3.1 Seismic hazard

PSHA was performed using the OpenQuake engine [8] based on the seismic hazard model ESHM13 [9] for a site in Duzce in Turkey. The analysis used a simplified logic tree with just a single ground motion model (AkkarEtAlRjb2014) [10] but kept the three logic tree branches to account for epistemic uncertainties in source characterisation. The analysis was carried out for ten return periods spanning 22 to 19,975 years, including 475 and 2475 years, to align with design code requirements. Outputs include hazard curves, as shown in Figure 4a, and the UHS previously shown in Figure 2 for 475-years return period. An example of seismic disaggregation is shown in Figure 4b for the 475-year return period.

Building	$\phi_y(m^{-1}) \times 10^{-3}$	$l_{pl}(m)$	$EI_{cr}(kN/m) \times 10^6$
4 Storey	1.8	0.70	14.7
8 Storey	1.0	1.22	90.56
12 Storey	0.7	1.75	278.52
16 Storey	0.6	2.18	463.99
20 Storey	0.5	2.63	818.48

Table 5. Building plastic hinge parameters

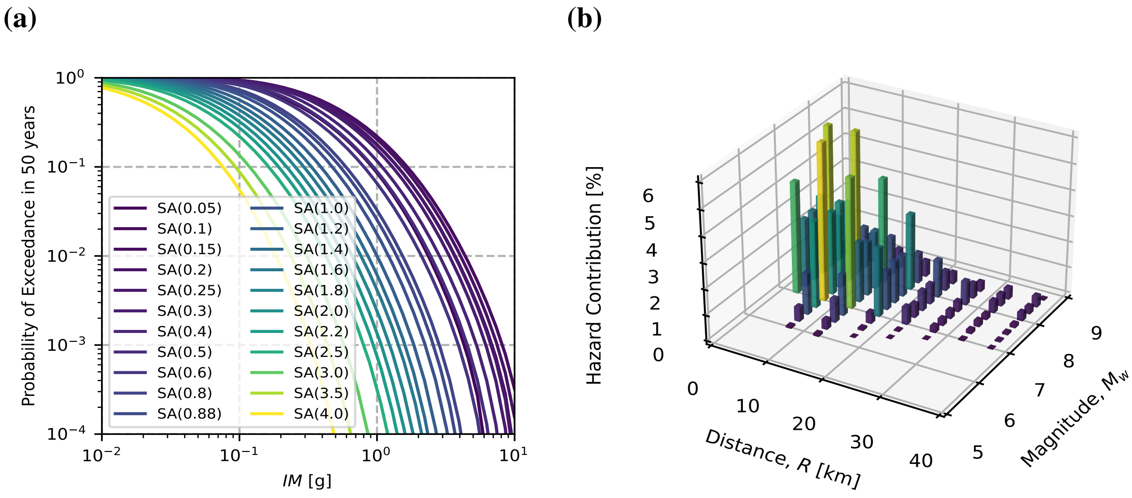

Fig. 4. a) Hazard curve; b) 475-year return period disaggregation for $Sa(T = 1.0s)$

3.2 Ground motion record selection

The record selection procedure involves selecting and scaling natural ground motions to match the target spectrum over the relevant range of periods. When selecting to match the UHS, records must closely match the mean spectrum within a specified tolerance, typically ±10% over the range $0.2(T_1)$ to $2.0(T_1)$ according to EC8 [4], for example, where T_1 is the fundamental period of the structure. The UHS-based selection is deemed to be equivalent to using the code-prescribed response spectrum in this study, as they are conceptually the same. Figure 5 presents the mean of the UHS-based record selection. Since this study encompassed five different buildings, the selection period range was extended from $0.05s$ to $4.0s$ to cover the 90% modal mass participation of the five buildings and the two times the first mode period rule for the 20-storey building, and the same UHS-based ground motions were adopted for all structures. For CS-based selection using $Sa(T)$, the ground motions are conditioned on a specific spectral acceleration value at a period $Sa(T^*)$ for the desired return period and also the variability of the ground motions at periods other than T^*. Unlike the UHS, the CS exhibits lower $Sa(T)$ at periods farther from the conditioning period. Constructing this spectrum requires PSHA disaggregation outputs and correlation models. Lin et al. [11] described the differences generated in CS when simplifications are applied, and in this case, the "exact" CS was used. For the CS-based selection, a wide range of T^* values ranging from $0.05s$ to $4.0s$ were selected, giving several different CS-based ground motion record sets all selected using slightly different conditioning choices. This is because an essential question in CS-based selection is determining the most appropriate conditioning period, T^*, for which several methodologies and recommendations exist in the literature [12], with the most common choice being the first mode period, $T* = T1$. This study comprehensively selected various conditioning periods to evaluate trends across different scenarios when periods other than the conditioning one were selected. As an example, Figure 5 shows a record selection for the conditional periods $Sa(T^* = 0.30s)$ and $Sa(T^* = 1.82s)$ alongside the UHS selection for the 475-year return period. It is evident that the spectral demands match between the CS and UHS at the conditioning period $T*$, but are lower at other periods. Given the multi-modal nature of RC shear wall response, it is the impact of this different that is of interest in this study.

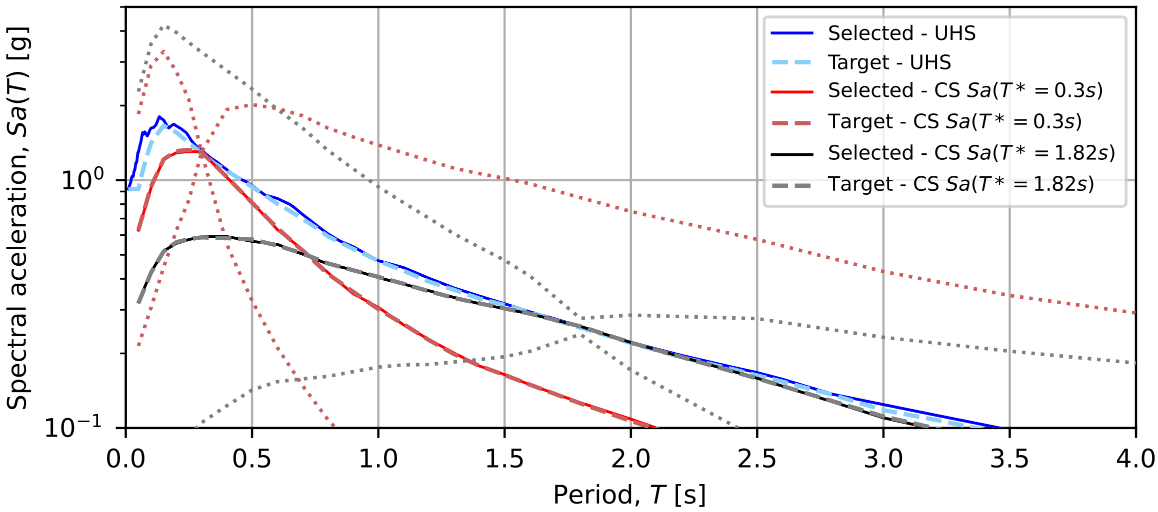

Fig. 5. 475-year return period UHS-based selection and CS-based selection for $Sa(T^* = 0.30s)$ and $Sa(T^* = 1.82s)$, where the target is plotted via dashed lines and the selected ground motions via the solid lines

The present study considers a single direction of analysis, so only one ground motion record is selected and used. Usually, building codes recommend between 7 and 11 records to assess the median of the structural response; for the present study, 40 ground motion records were selected per return period.

3.3 Multiple stripe analysis

Multiple Stripe Analysis (MSA) is a method in earthquake engineering that involves the analysis of a structural model with multiple ground motion records, each scaled to a specific intensity measure, such as spectral acceleration at a given period. This study analysed 40 ground motion records for the ten return periods analysed in PSHA. In total, 9,200 scaled records were evaluated, derived from 40 records across 10 return periods and 23 target spectra (22 conditional spectra and one uniform hazard spectrum). This comprehensive analysis thus aims to provide insights into the effects of record selection on EDPs used to describe RC shear wall performance subsequent design. For example, 6 illustrates the median (non-collapsed) response for UHS-based and two CS-based selection at the 475-year return period for the 20-storey building and compared to the capacity design envelope. The CS-based selections were done with the first and second mode conditional periods, meaning $Sa(T^* = T_1)$ and $Sa(T^* = T_2)$, respectively. Examining the storey drift demands, it is evident that the CS conditioned on T_1 quite closely resembles the UHS-based demand, underlining the first-mode dominance of displacement-based EDPs, whereas the CS conditioned on T_2 tends to underestimate the drift demand. Hence, if an analyst wished to move away from the conceptual inconsistencies of the UHS and utilise hazard-consistent ground motions via the CS, conditioning on T_1 appears to be a logical choice. Examining the shear force and bending moment demands, it is clear that the CS conditioned on T_1 quite closely resembles the UHS-based demand in the lower half of the wall, but underestimates the demands in the upper half because of the lack of higher mode contributions due to the lower spectral demands at those shorter periods. Likewise, the CS conditioned on T_2 underestimates the demands in the lower half but aligns well with the

UHS in the upper half of the wall because the higher mode spectral demands are more closely aligned with the UHS. Hence, if an analyst were to choose the CS-based approach, the results would be highly dependent on which conditioning period is selected, with the consequence that the demands will be underestimated in one part of the wall, which would be problematic for ensuring capacity design. These results refer to a single structure at a single return period intensity. The following section discusses the results for all structures in a more general manner.

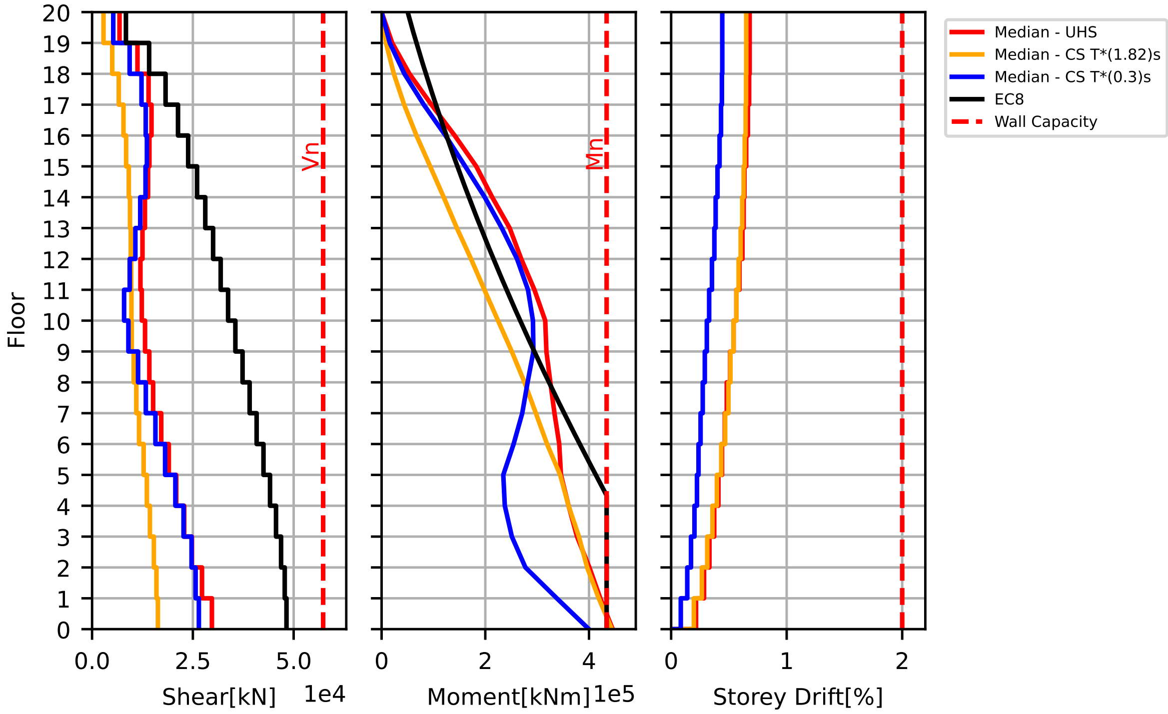

Fig. 6. Median (non-collapsed) analysis results at the 475-year return period using UHS-based selection, CS-based selection at $Sa(T^* = 1.82s)$ and $Sa(T^* = 0.3s)$

4 Results

The primary objective of this study is to compare key EDP values for RC shear walls obtained using different record selection methods. Figure 7 presents what are termed *EDP spectra* herein for each building by plotting the EDPs of interest as a function of the conditional period T^* used in CS-based selection. For comparison, the UHS-based selection is shown as a constant, since it is invariant to the conditioning period. To maintain clarity, results are presented for only two return periods: 475 and 2475 years. For shear demands, the median base shear demand is normalised by the maximum demand from the capacity design envelope ($V_{Ed,b}$ in Table 4). Similarly, for moment demands, the median base overturning moment demand is normalised by the maximum demand from the capacity design envelope (M_n in Table 4). For drifts, the drift at the top of each building is normalised by the 2% drift limit prescribed in the code. These normalisations help illustrate whether the demands exceed the design envelope or the drift limit on relative terms. The vertical lines in the EDP spectra represent the first three structural modes for each building (i.e., T_1, T_2 and T_3), providing insight into the correlation between structural modes and the corresponding structural responses. Finally, Table 6 presents the ratio between UHS-based selection and the peak of all CS-based selection at 475- and 2475-year return periods. These ratios helps understand how UHS-selection relates to CS-selection for different EDPs. Discussion of these results is presented in the following subsections analysing one EDP at a time.

	475-year return period			2475-year return period		
Building	Shear	Moment	Drift	Shear	Moment	Drift
4 Storey	1.03	1.02	1.10	1.05	1.03	1.10
8 Storey	1.01	1.01	1.05	1.07	1.02	1.09
12 Storey	1.12	1.00	1.06	0.99	1.01	1.09
16 Storey	1.02	0.99	0.98	0.99	1.00	1.08
20 Storey	1.12	0.99	0.99	1.04	1.00	1.00

Table 6. Ratio of the UHS demand to the peak of the CS demands

4.1 Shear demands

For the shear demands, Figure 7 shows these ratios in the left column of plots for each building. Starting with the UHS-based assessment, which represents the standard approach adopted in building codes, the capacity design provisions generally provide adequate capacity at the 475-year return period. Only the 4-storey building exhibits a slightly higher ratio of 1.06. In contrast, the CS-based assessment offers additional insights into shear demand. Peak shear demands at the wall's mid-height are observed at the building's second mode-based selection, $Sa(T^* = T_2)$. On average, the first mode selection, $Sa(T^* = T_1)$, generates 62% of the peak base shear demand for all buildings, from the $Sa(T^* = T_2)$ demand at the 475-year return period, while the third mode selection, $Sa(T^* = T_3)$, generates 85% of the peak base shear demand from the $Sa(T^* = T_2)$ base shear demand. Linking the peak values from CS-based and UHS-based assessments (as shown in Table 6), it is noteworthy that the UHS selection produces demands in the structure that are higher than those of the CS selection by an average ratio of 1.06. From the CS-based selections, it is evident that the second mode selection contributes most significantly to shear demands in all structures. This indicates that selecting a conditional period based on the first mode T_1 would substantially underpredict shear demands. This is noteworthy because the current EC8 draft [3] fixes the conditional period to the first fundamental mode, T_1. In contrast, ASCE7-22 [13] mandates the use of at least two conditional periods, defined as periods that significantly contribute to the inelastic dynamic response in the two orthogonal directions. Additionally, ASCE7-22 [13] sets a lower bound for the mean of the CS targets at 75% of the UHS, ensuring higher mode effects are reasonably accounted for if the selected conditional periods fail to do so. These issues must be clear to practitioners and governed correctly in the code prescriptions because lack of clear guidance and practical instruction can lead the actual demands being substantially underestimated, despite analysts using what is touted as a much more sophisticated and accurate ground motion selection strategy. While the second mode CS-based selection $T^* = T_2$ captures shear response more realistically than UHS-based selection due to its explicit correlation with spectral intensities, it requires an additional set of ground motions beyond the standard $T^* = T_1$ selection. On the other hand, although UHS-based selection tends to overpredict maximum shear demands by a maximum of 1.12 (as shown in Table 6), it only requires one set of ground motions.

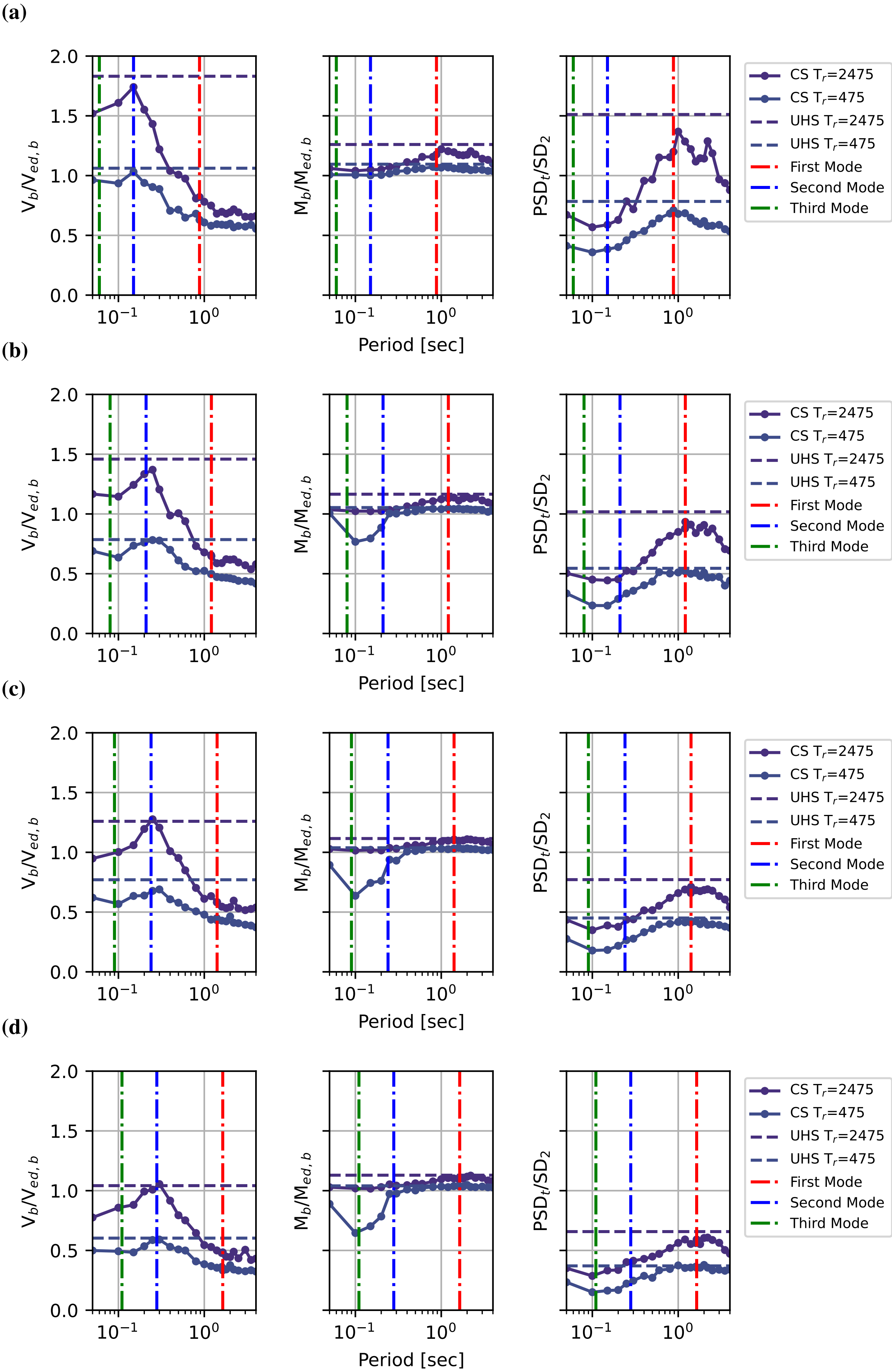

Fig. 7. EDP spectra for 475 and 2475-year return periods (Part 1), a) 4-storey building; b) 8-storey building; c) 12-storey building; d) 16-storey building

(e)

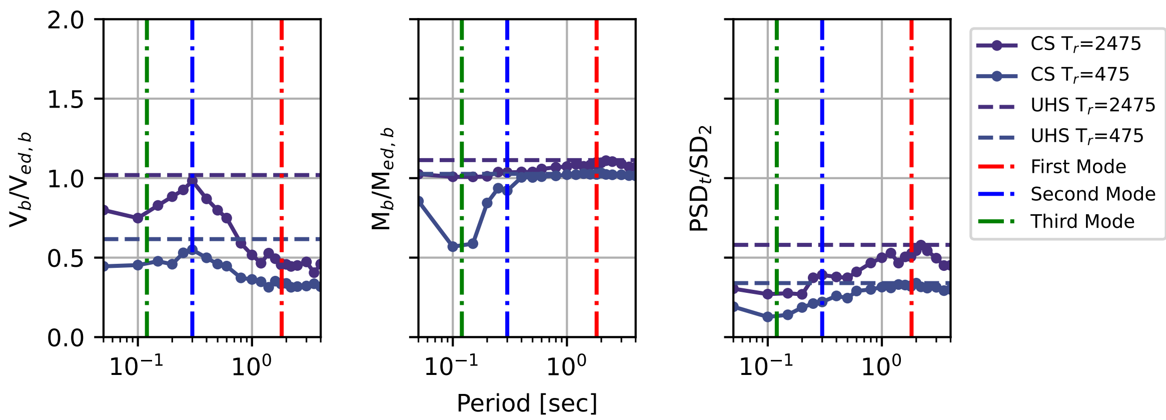

Fig. 7. EDP spectra (Part 2), e) 20-storey building

4.2 Moment demands

For overturning moments in Figure 7, the UHS-based selection at the 475-year return period indicates that yielding is achieved. Given the model's 1% post-yielding positive flexural stiffness, further increases in demand, as 2475-year return period, do not increase significantly the ratios. Similar to shear demands, the CS-based assessment provides additional insights into moment demand behaviour. At the 475-year return period, the conditional period selections capable of inducing flexural yielding range from values near the second mode ($Sa(T^* = T_2)$) to periods longer than the first mode ($Sa(T^* > T_1)$). This indicates that high moment demands at the base are not solely associated with the first mode (T_1) or its elongated equivalent ($> T_1$)). Notably, a pronounced dip in moment demands is observed near the third mode ($Sa(T^* = T_3)$) at the 475-year return period. However, at higher intensities, such as the 2475-year return period, even the third mode selection ($Sa(T^* = T_3)$) can induce yielding at the base.

4.3 Peak storey drift demands

For peak storey drifts in Figure 7, the drift limit of 2% is not exceeded for neither the 475-year nor the 2475-year return periods, except for the 4-storey building. A strong correlation is observed between the drift demands resulting from the ground motions selected to match the UHS and those selected based on the CS at the first mode, $Sa(T^* = T1)$, and slightly longer periods, $Sa(T^* > T_1)$. This further underlines the fact that drift demands in structures tend to be dominated by the first mode of response. This is because the demands of the $Sa(T^* = T_1)$-based selection, whose $Sa(T_2)$ values will be much lower than the UHS-based selection, coincide well with the UHS-based selection, where they are equal (i.e., $Sa(T_1)_{CS} \approx Sa(T1)_{UHS}$ and $Sa(T_2)_{CS} < Sa(T_2)_{UHS}$). Compared to the previous sections discussed on force-based demands (i.e., shear and moment), it highlights that a CS-based record selection conditioned on the first mode period is likely to give very similar, if not slightly lower, drift demands compared to the UHS-based selection. This is both reassuring for analysts as they would now be using ground motions that are hazard-consistent, and not conservative and somewhat unrealistic like the UHS-based ones [14]. The ratio between the demands of the UHS-based selection and the maximum CS-based selection drifts tends to increase for shorter buildings, with the UHS-based selection overpredicting drifts by up to a factor of 1.1. For taller buildings, this discrepancy diminishes, with the ratio approaching 1.0 for the 16- and 20-storey structures.

4.4 Capacity design envelopes

Additionally, apart from the key EDP values, it is noteworthy how the capacity design envelopes align with the actual response of the structures. For example, Figure 6 compares median non collapse demands for the 20-storey building at 475-year return period. This alignment is crucial, as it can inform design optimisations along the height of the structures based on these envelopes. For the UHS-based selection, which is generally conservative, the shear capacity envelope is higher throughout the height of the building compared with the EC8 capacity design envelope. However, the shapes differ, with the median shear demands spiking at the upper floors due to higher mode effects. For bending moments, the UHS-based selection shows median demands exceeding the capacity envelope at mid-height, highlighting a potential yielding location if the design optimisation closely follows the capacity design envelope and ductile detailing required. Finally, comparing shear and moment shapes for UHS- and CS-based selections, it is evident that UHS selection serves as an envelope for the CS-based selections. Notably, the UHS selection captures higher modes effects, including spikes of shear and moment at higher floors.

5 Conclusions

This study investigated the seismic performance of RC shear wall buildings subjected to ground motion records selected using Uniform Hazard Spectrum (UHS) and Conditional Spectrum (CS) approaches. Key Engineering Demand Parameters (EDPs), including shear, bending moment, and peak storey drift, were analysed for structures of varying heights at mainly two return periods (475 and 2475 years). The results highlighted the influence of higher modes in shear demands, the limitations and comparative performance of UHS- and CS-based selection. Below is a summary of the key findings:

- The CS-based assessment reveals that the shear demands in the upper half of the walls occur at the second mode selection, $Sa(T^* = T_2)$, with first mode selection $Sa(T^* = T_1)$, reaching a 62% and third mode selection $Sa(T^* = T_3)$, reaching 85% of the peak demand at the base on average.

- The UHS-based selection captures higher mode effects well but tends to overpredict maximum shear demands compared to $Sa(T^* = T_1)$ selection, with an average overestimation factor of 1.06.

- CS-based assessments show that moment demands capable of inducing yielding range from second mode periods to those longer than the first mode, suggesting that base moments are not exclusively tied to the first mode.

- Drift demands are primarily dominated by the first mode with strong agreement between UHS- and $Sa(T^* = T_1)$ selection.

- UHS-based selection serves as a natural envelope for CS-based selections, effectively capturing higher mode effects, including shear and moment spikes at upper floors, but nevertheless suffer the conceptual issues with its hazard consistency and definition.

This study primarily focused on the provisions of Eurocode 8, as the next generation of the code is set to be published. A notable new feature in the draft is the introduction of CS-based record selection, but the conditional period is currently restricted to the first fundamental mode,

T_1. Based on the findings of this study and similar analyses in the existing literature [12], it is recommended to at least include a second CS-based record selection associated with the second mode period, $Sa(T^* = T_2)$. Similarly, ASCE 7-22 [13] included similar recommendation, advocating for the use of two or more conditional period selections and stipulating a lower bound of 75% of the UHS for the mean envelope of CS-based selections. While these provisions offer improvements in accuracy, they may introduce significant complexity and potentially discourage the adoption of CS-based record selection methods. Nonetheless, the CS-based selection method should be promoted for its hazard consistency [2] and potential economic benefits [12], as it demonstrated lower shear demands compared to the UHS selection.

6 Acknowledgements

The work presented in this paper has been developed within the framework of the project "Dipartimenti di Eccellenza 2023-2027," funded by the Italian Ministry of Education, University and Research at IUSS Pavia. We thank for the academic license from www.djura.it, used to perform the ground motion record selection.

References

[1] Rosita Jünemann et al. "Study of the damage of reinforced concrete shear walls during the 2010 Chile earthquake". In: *Earthquake Engineering and Structural Dynamics*. Vol. 45. 10. John Wiley and Sons Ltd, Aug. 2016, pp. 1621–1641. DOI: 10.1002/eqe.2750.

[2] Ting Lin et al. "Conditional spectrum-based ground motion selection. Part I: Hazard consistency for risk-based assessments". In: *Earthquake Engineering and Structural Dynamics* 42.12 (Oct. 2013), pp. 1847–1865. ISSN: 10969845. DOI: 10.1002/eqe.2301.

[3] CEN/TC 250. *Eurocode 8 - Design of structures for earthquake resistance - Part 1-1: General rules and seismic action*. Tech. rep. 2023.

[4] CEN. *Eurocode 8, design of structures for earthquake resistance. Part 1, General rules, seismic actions and rules for buildings*. British Standards Institution, 2005, p. 229. ISBN: 0580458725.

[5] Shahen Akelyan and Gregg Brandow. *AN ALTERNATIVE PROCEDURE FOR SEISMIC ANALYSIS AND DESIGN OF TALL BUILDINGS AN ALTERNATIVE PROCEDURE FOR SEISMIC ANALYSIS AND DESIGN OF TALL BUILDINGS 2023 Edition A consensus document developed by the Council Council Active Members*. Tech. rep. 2023.

[6] Frank McKenna. *OpenSees: A Framework for Earthquake Engineering Simulation*. Tech. rep. 2011.

[7] M.J.N. Priestley et al. *Displacement Based Seismic Design of Structures*. Ed. by IUSS Press. IUSS Press, 2007. ISBN: 978-88-6198-000-6. URL: www.iusspress.it.

[8] Marco Pagani et al. "OpenQuake engine: An open hazard (and risk) software for the global earthquake model". In: *Seismological Research Letters* 85.3 (2014), pp. 692–702. ISSN: 1938-2057.

[9] Jochen Woessner et al. "The 2013 European Seismic Hazard Model: key components and results". In: *Bulletin of Earthquake Engineering* 13.12 (Dec. 2015), pp. 3553–3596. ISSN: 15731456. DOI: 10.1007/s10518-015-9795-1.

[10] S. Akkar et al. "Empirical ground-motion models for point- and extended-source crustal earthquake scenarios in Europe and the Middle East". In: *Bulletin of Earthquake Engineering* 12.1 (Feb. 2014), pp. 359–387. ISSN: 15731456. DOI: 10.1007/s10518-013-9461-4.

[11] Ting Lin et al. "Conditional spectrum computation incorporating multiple causal earthquakes and ground-motion prediction models". In: *Bulletin of the Seismological Society of America* 103.2 A (Apr. 2013), pp. 1103–1116. ISSN: 00371106. DOI: 10.1785/0120110293.

[12] Tamika J. Bassman et al. "Evaluation of Conditional Mean Spectra Code Criteria for Ground Motion Selection". In: *Journal of Structural Engineering* 148.11 (Nov. 2022). ISSN: 0733-9445. DOI: 10.1061/(asce)st.1943-541x.0003471.

[13] ASCE/SEI 7-22. *Minimum Design Loads and Associated Criteria for Buildings and Other Structures*. Reston, VA: American Society of Civil Engineers, Nov. 2021. ISBN: 9780784415788. DOI: 10.1061/9780784415788.

[14] Julian J. Bommer and Rui Pinho. "Adapting earthquake actions in Eurocode 8 for performance-based seismic design". In: *Earthquake Engineering and Structural Dynamics* 35.1 (2006), pp. 39–55. ISSN: 00988847. DOI: 10.1002/eqe.530.